Full Articles

Combinatorial-topological modeling of the cluster self-assembly of zeolite crystal structures: computer search for molecular templates for new zeolite ISC-2*

V. Ya. Shevchenko,[a] A. A. Golov,[b] V. A. Blatov,[b] and G. D. Ilyushin[b,c]*

[a]*I. V. Grebenshchikov Institute of Silicate Chemistry, Russian Academy of Sciences, 2 nab. Makarova, 199034 St.-Petersburg, Russian Federation. E-mail: shevchenko@isc.nw.ru*

[b]*Samara Center for Theoretical Materials Science, Samara State University, 1 ul. Akad. Pavlova, 443011 Samara, Russian Federation.*

[c]*A. V. Shubnikov Institute of Crystallography, Russian Academy of Sciences, 59 Leninskii prosp., 119333 Moscow, Russian Federation*

The combinatorial-topological modeling of 3D periodic packings of layers composed of T_{12} polyhedral clusters (**t-hpr** tiles in the form of hexagonal prisms) was carried out. The T_{12} clusters are among the most abundant units in the crystal structures of zeolites. The layers were produced by decoration of the vertices of the square and hexagonal (graphite-like) nets with T_{12} clusters. All combinatorially possible patterns of 3D frameworks, which were constructed based on packings of decorated square nets, correspond to known zeolite structures: **CHA** (mineral chabazite, $Ca_6(H_2O)_{40}Al_{12}Si_{24}O_{72}$), **AEI** (AlPO-18, $Al_{24}P_{24}O_{96}$), **SAV** ($(C_{18}H_{42}N_6)_2(H_2O)_7Mg_5Al_{19}P_{24}O_{96}$), and **KFI** ($Na_{30}(H_2O)_{98}Al_{30}Si_{66}O_{192}$). The modeling using the same scheme and a decorated hexagonal net gave rise to the frameworks of three known zeolites, **GME** (gmelinite, $(Ca,Na)_4(H_2O)_{24}Al_8Si_{16}O_{48}$), **AFX** (SAPO-56, $H_3Al_{23}Si_5P_{20}O_{96}$), and **AFT** (AlPO-52, $Al_{36}P_{36}O_{144}$), as well as of one previously unknown hypothetical zeolite **ISC-2** with the unit cell parameters a = 13.90 Å, c = 30.00 Å, V = 5019.7 Å^3, sp. gr. $P\bar{6}m2$. Zeolite **ISC-2** contains a cavity with a new **t-isc-2** topology [$4^{21}.6^2.8^{15}$], which is responsible for its unique framework. An analysis of the specially created database of topological types of molecules (TTM collection) containing geometric and topological characteristics of more than 300000 different molecules suggested an organic structure-directing agent, which stabilizes the **t-isc-2** cavity and which can be used for the synthesis of **ISC-2**.

Key words: zeolites, self-assembly of crystal structures, mathematical modeling.

* Dedicated to Academician of the Russian Academy of Sciences N. S. Zefirov on the occasion of his 80th birthday.

There are currently 225 topologically different 3D zeolite frameworks[1] characterized by three-periodic 3D nets

Published in Russian in *Izvestiya Akademii Nauk. Seriya Khimicheskaya,* No. 1, pp. 0029—0039, January, 2016.

1066-5285/16/6501-0029

composed of tetrahedrally coordinated atoms (T nets) as the structural model. The construction of each new framework type presents a challenge. Not more than 3—5 new zeolite frameworks are synthesized annually worldwide. Therefore, the modeling of the self-assembly of zeolite structures from known polyhedral building units is of utmost importance.[1—5] According to the statistical data,[4—7] the T_{12} polyhedral cluster in the form of the hexagonal prism **t-hpr** is most frequently observed in 3D zeolite T-nets. In some crystal structures of zeolites, the T_{12} cluster contains all crystallographically independent T-nodes of the framework and it is the only structural building unit, the packing of which is completely responsible for the topology of the overall 3D zeolite net.[6—9] Earlier, we have considered the following models of the cluster self-assembly of the zeolite structure: with the **CHA** framework (chabazite, $Ca_6Al_{12}Si_{24}O_{72}(H_2O)_{40}$ and willhendersonite, $Ca_2K_2Al_6Si_6O_{24}(H_2O)_{10}$) from templated T_{12} clusters,[8] with the **PAU** framework (paulingite, $Na_{13}Ca_{36}K_{68}Ba_{1.5})Al_{152}Si_{520}O_{1344}$ wH_2O) from three clusters, T_6, T_{16}, and T_{20},[9] with the **LTN** framework ($Na_{384}Al_{384}Si_{384}O_{1536}(H_2O)_{422}$) from two clusters, T_{24} and T_{48},[10] and with the **CAN** framework (cancrinite, $Na_8(Al_6Ge_6O_{24})Ge(OH)_6(H_2O)_2$ and $Cs_2Na_6(Al_6Ge_6O_{24})Ge(OH)_6$) from T_6 clusters.[11] The modeling of zeolites[8—11] resulted in the reconstruction of the following symmetrical-topological code of the self-assembly processes of 3D structures from clusters: 1D primary chain → 2D microlayer → 3D microframework.

The aim of the present study was to perform for the first time the combinatorial-topological modeling of the packings from symmetry-related T_{12} polyhedral clusters taking the shape of hexagonal prisms that form symmetrically nonequivalent 2D layers, which are then assembled to the zeolite framework. This modeling would provide an explanation of the known zeolite structures and predict the possibility of the formation of new framework types. An organic structure-directing agent is proposed for a new zeolite framework type. This agent can be used in the synthesis of the latter zeolite.

The present study is a continuation of investigations[8—19] in the field of geometric and topological analysis of the structures of crystalline phases and the modeling of the self-organization of chemical systems by means of modern computer methods.[20]

Results and Discussion

Geometric and topological modeling of the packings assembled from T_{12} clusters (hexagonal prisms)

The T_{12} polyhedral cluster in the form of a hexagonal prism serves as a topological model of the cluster structure composed of 12 T-tetrahedra (Fig. 1).

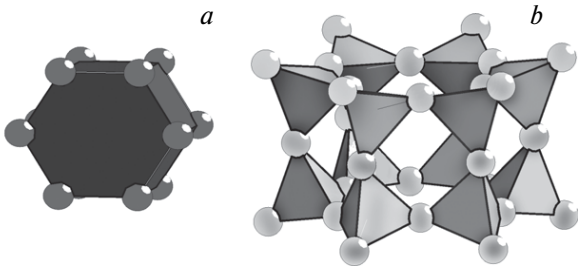

Fig. 1. The T_{12} cluster monomers; *a*, a topological model of the structure represented as a 12-node hexagonal prism; *b*, a cluster comprising 12 TO_4 tetrahedra.

The symmetry of the T_{12} cluster is described by the symmetry point group $\bar{6}m2$. The T_{12} clusters are connected to each other by T—O—T bridges to form supraclusters. Therefore, any supracluster is a packing of connected clusters, which do not share T-nodes. Let us consider the topological mechanisms of the formation of supraclusters of different complexity giving rise to the overall zeolite framework.

Supracluster dimer $(T_{12})_2$. The T_{12} clusters are involved in the primary (random) connection to each other to form dimers or primary chains (Fig. 2). The $T_{12} + T_{12}$ clusters can be connected in the following ways characterized by the local connectivity index P_{loc}, the value of which is equal to the number of bridges between the clusters:

— *via* six lateral edges of the prism ($P_{loc} = 2$);

— *via* twelve edges in the base of the prism ($P_{loc} = 2$);

— *via* six lateral square faces of the prism ($P_{loc} = 4$);

— *via* six lateral square faces of the prism followed by the rotation and formation of two additional linkages between the clusters ($P_{loc} = 4 + 2 = 6$);

— *via* two hexagonal faces lying in the base of the prism ($P_{loc} = 6$).

The presence of two, four, and six bridges in the dimers that held the $T_{12} + T_{12}$ monomers in a certain position serves as the basis for the unambiguous classification of these interactions with an indication of the point symmetry of the dimer ($g = m$, -1, or 2).

Supraclusters as 2D microlayers based on underlying square nets and their packings in 3D frameworks. The next hierarchical level in the self-assembly process of the zeolite framework in terms of the model under consideration involves the assembly of dimers to form $(T_{12})_4$ tetramers as fragments of layered supraclusters. Such microlayers can be produced by decoration of the underlying square 2D net. There are the following three combinatorially possible ways of formation of such microlayers:

1. The **L1** microlayer ($-1,-1$). Centrosymmetric dimers ($g = -1$) are related by a center of symmetry. The unit cell of the microlayer is characterized by equal vectors of two independent translations (Fig. 3, *a*).

2. The **L2** microlayer ($-1, m$). Centrosymmetric dimers are related by a mirror plane *m*. In this case, the unit cell of

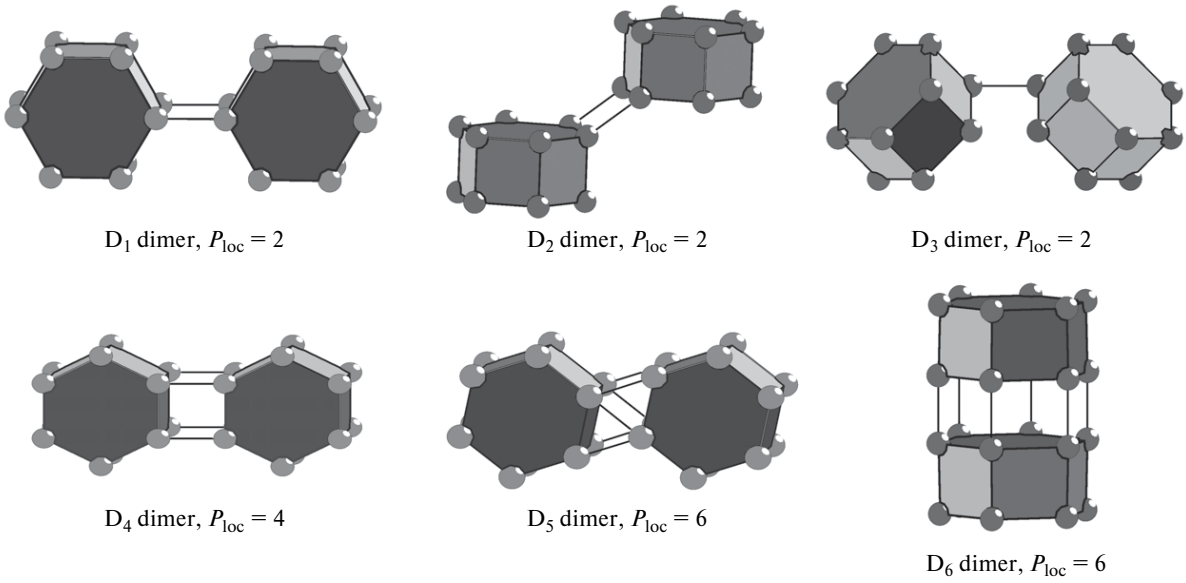

Fig. 2. Dimers T_{12}+T_{12}.

the microlayer has a doubled translation vector perpendicular to the mirror plane (see Fig. 3, *b*).

3. The **L3** microlayer (*m*, *m*). In this case, the monomers in the dimers, as well as the dimers by themselves, are related by mirror planes, and both translation vectors of the unit cell of this microlayer are doubled (see Fig. 3, *c*).

A microlayer, in which dimers having a mirror plane are related by a center of symmetry is equivalent to the **L2** microlayer.

Let us consider the combinatorially possible ways of self-assembly of 3D microframeworks (octamers) from two equivalent **L1**, **L2**, or **L3** 2D microlayers. It should be noted that the connectivity mode of two microlayers in a microframework can be characterized by a secondary microlayer perpendicular to the former two microlayers, which can always be distinguished in such microframeworks. As it is shown below, this layer is in all cases topologically equivalent to one of the underlying **L1**—**L3** microlayers. The correspondence of the structures to known zeolites (Table 1) was established using the ToposPro program package.[20]

The **FR-1** microframework was produced by the self-assembly of the **L1** microlayers related by a center of symmetry $g = 1$ (Fig. 4, *a*); it topologically corresponds to the framework of zeolite **CHA** (mineral chabazite, $Ca_6(H_2O)_{40}Al_{12}Si_{24}O_{72}$).[1] The secondary microlayer also has the **L1** topology. The unit cell of the 3D framework is characterized by equal translation vectors, and its volume has the minimum possible value ($V_{cell} = V_0$) (see Fig. 4, *a*, Table 1).

The **FR-2** microframework was generated by assembling the **L1** microlayers related by a mirror plane (see Fig. 4, *b*). It corresponds to synthetic zeolite **AEI** (AlPO-18, $Al_{24}P_{24}O_{96}$),[1] the secondary microlayer having the **L2** topology.

The **FR-3** microframework was produced by the self-assembly of the **L3** microlayers related by a center of symmetry (see Fig. 4, *c*); the secondary microlayer has the **L2**

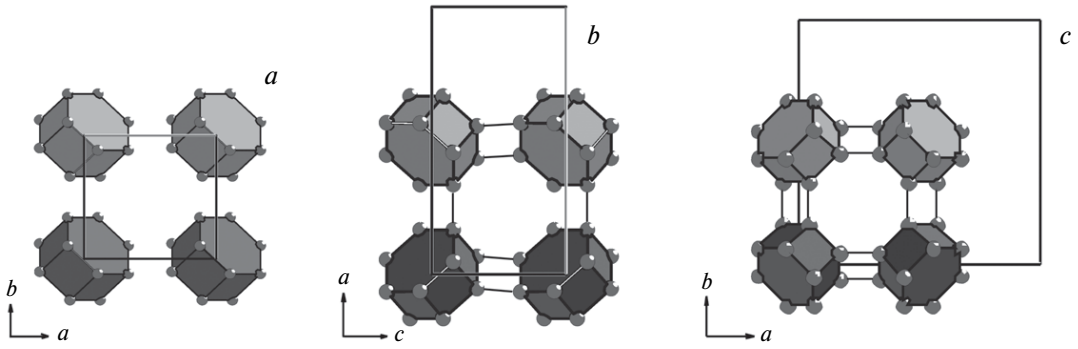

Fig. 3. The $(T_{12})_4$ microlayers derived by decoration of the underlying square 2D net 4.4.4.4: *a*, **L1** microlayer (−1, −1); *b*, **L2** microlayer (−1, *m*); *c*, **L3** microlayer (*m*, *m*).

Table 1. Crystal-structural data for the frameworks, the type and symmetry of the crystal-forming structural units

Framework type	Symmetry group	Symmetry			Note
		T_{12} cluster	C chain	L microlayer	
		CHA family			
CHA	$R\bar{3}m$	$\bar{3}m$ (3*a*)	C2, $g = \bar{1}$	**L1**, $g = \bar{1}$	$V_{cell} = V_0$
AEI	*Cmcm*	2/*m* (4*a*)	C2, $g = \bar{1}$	**L1**, $g = \bar{1}$	$V_{cell} = 2\ V_0$
SAV	*P*4/*nmm*	2/*m* (4*d*)	C3, $g = m$	**L3**, $g = m$	$V_{cell} = 4\ V_0$
KFI	$Im\bar{3}m$	$\bar{3}m$ (8*c*)	C3, $g = m$	**L3**, $g = m$	$V_{cell} = 8\ V_0$
		GME family			
GME	$P6_3/mmc$	$\bar{6}m2$ (2*d*)	C8	L12	1L-polytype
AFX	$P6_3/mmc$	$\bar{6}2$ (2*a*, 2*c*)	C8	L12	2L-polytype
AFT	$P6_3/mmc$	$\bar{6}2$ (2*b*), 3*m* (4*f*)	C8	L12	3L-polytype
FR-8 (ISC-2)	$P\bar{6}m2$	$\bar{6}m2$ (1*b*, 1*c*), 3*m* (2*h*, 2*i*)	C8	L12	3L-polytype

topology. There is an equivalent self-assembly pattern for this framework from the **L2** layers related by the plane *m*. The framework corresponds to synthetic zeolite **SAV** $((C_{18}H_{42}N_6)_2(H_2O)_7Mg_5Al_{19}P_{24}O_{96})$**1** (see Table 1).

The **FR-4** microframework was generated by the self-assembly of the **L3** microlayers related by a mirror plane (see Fig. 4, *d*); the secondary layer is topologically also equivalent to **L3**. The structural model of the frame-

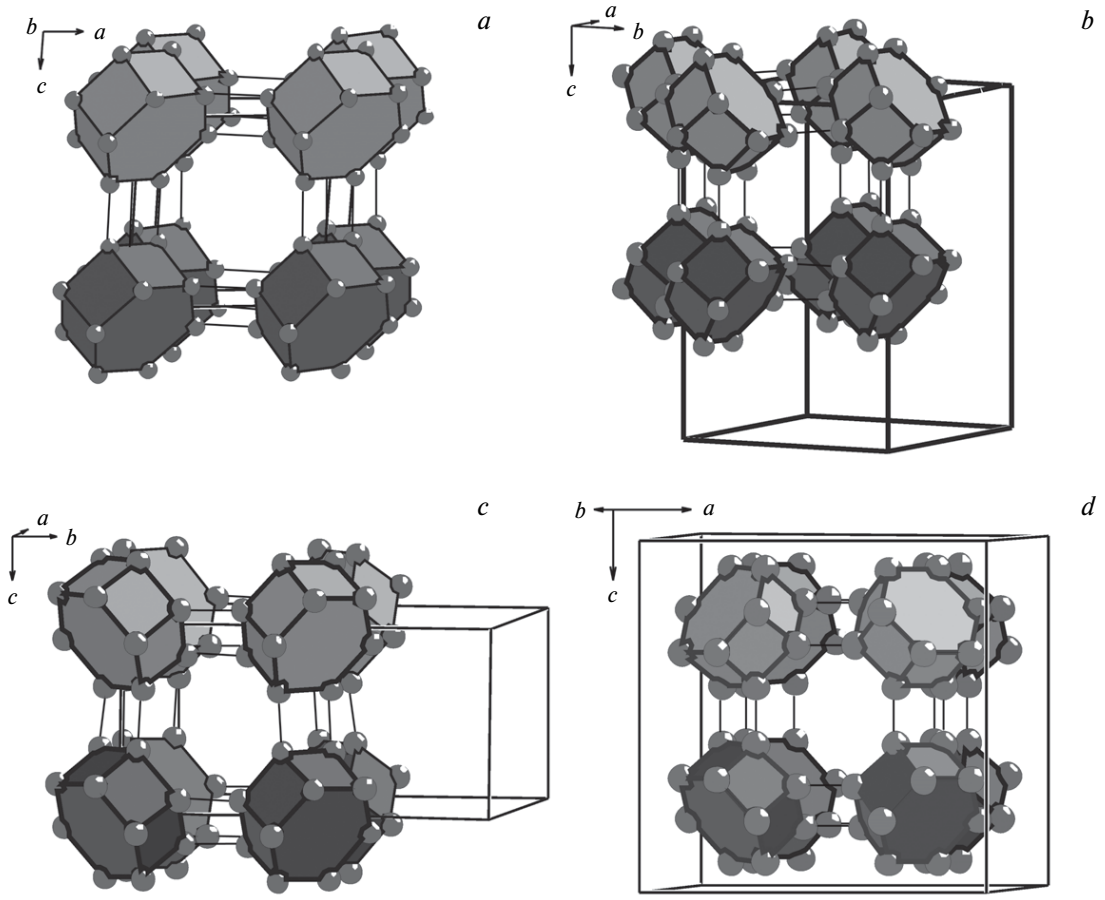

Fig. 4. Self-assembly of the frameworks from two $(T_{12})_4$ microlayers: *a*, **L1** (cha, −1, −1), **FR-1** framework, **CHA** structure type; *b*, **L1** (cha, −1, −1), **FR-2** framework, **AEI** structure type; *c*, **FR-3** framework, **SAV** structure type; *d*, **FR-4** framework, **KFI** structure type.

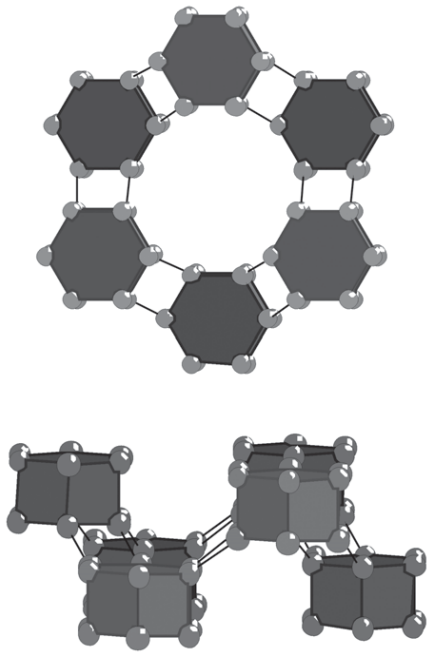

Fig. 5. The $(T_{12})_6$ cluster hexamer (two projections).

work corresponds to synthetic zeolite **KFI** ($Na_{30}(H_2O)_{98}$-$Al_{30}Si_{66}O_{192}$)[1] (see Table 1). Therefore, all combinatorially possible structures of zeolite frameworks composed of layers based on underlying square nets correspond to real zeolite structures.

Supraclusters as of 2D microlayers based on underlying hexagonal nets and their packings in 3D frameworks. Let us consider the formation of microlayers having hexagonal symmetry, which can be produced by decoration of graphite-like nets and are composed of six T_{12} clusters (Fig. 5).

The formation of an infinite number of polytype structures is theoretically possible due to different types of the complementary arrangement of the layers connected to each other. Figure 6 shows three possible connectivity modes for $(T_{12})_6$ hexamers. These modes are characterized by the sum-connectivity index (P_{sum}), which is equal to the number of linkages that are formed between the microlayers upon self-assembly of the microframework:

1) the upper $(T_{12})_6$ hexamer is located above the lower hexamer without displacement ($P_{sum} = 12$);

2) the upper $(T_{12})_6$ hexamer is located above the lower hexamer with displacement ($P_{sum} = 10$), the T_{12} cluster located above the center of the lower cluster having no linkages with it;

3) the upper $(T_{12})_6$ hexamer is located above the lower hexamer with displacement ($P_{sum} = 10$), the T_{12} cluster located above the center of the lower cluster forming linkages with it.

The above-considered arrangement patterns of the microlayers give rise to the following types of microframeworks.

The **FR-5** microframework is produced from the $(T_{12})_6$ hexamers located one above another according to pattern 1 and contains through channels (Fig. 7). The model corresponds to the **GME** framework (gmelinite, $(Ca,Na)_4(H_2O)_{24}Al_8Si_{16}O_{48}$)[1] (see Table 1). In the crystal structure, the microlayers are related by translations ($c \approx 10$ Å). The **GME** structure type can be classified as a single-layer 1L structure serving as the basis of the abundant family of *N*L-polytype structures with the hexagonal unit cell parameters: $a = 13.75$ Å, $c \approx N \cdot 10$ Å.

The **FR-6** microframework was generated by the self-assembly of $(T_{12})_6$ hexamers with displacement according to arrangement pattern 2 (Fig. 8). The structural model of the framework corresponds to the **AFX** framework (SAPO-56, $H_3Al_{23}Si_5P_{20}O_{96}$)[1] (see Table 1), which is classified as the 2L-polytype of the **GME** family; $c \approx 2 \cdot 10$ Å.

The **FR-7** microframework was generated by the self-assembly of $(T_{12})_6$ hexamers with displacement according to arrangement patterns 2 and 3 (Fig. 9). The structural model of the framework corresponds to the **AFT** framework (AlPO-52, $Al_{36}P_{36}O_{144}$)[1] (see Table 1). This is the 3L-polytype of the **GME** family with the translation $c \approx 3 \cdot 10$ Å.

Finally, the **FR-8** microframework can be produced by a combination of arrangement patterns 1 and 3 (Fig. 10). The structural model of this framework, which we called

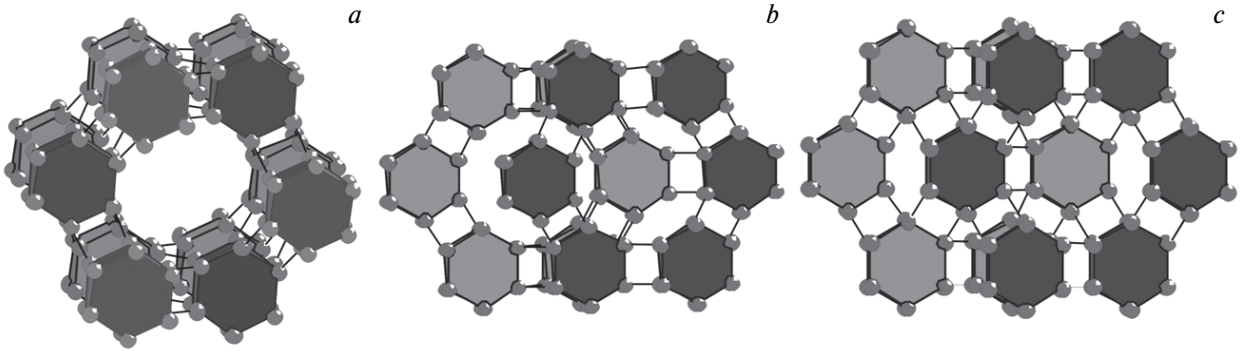

Fig. 6. Mechanism of assembling of $(T_{12})_6$ hexamers: *a*, pattern 1, $P_{sum} = 12$; *b*, pattern 2, $P_{sum} = 10$; *c*, pattern 3, $P_{sum} = 10$.

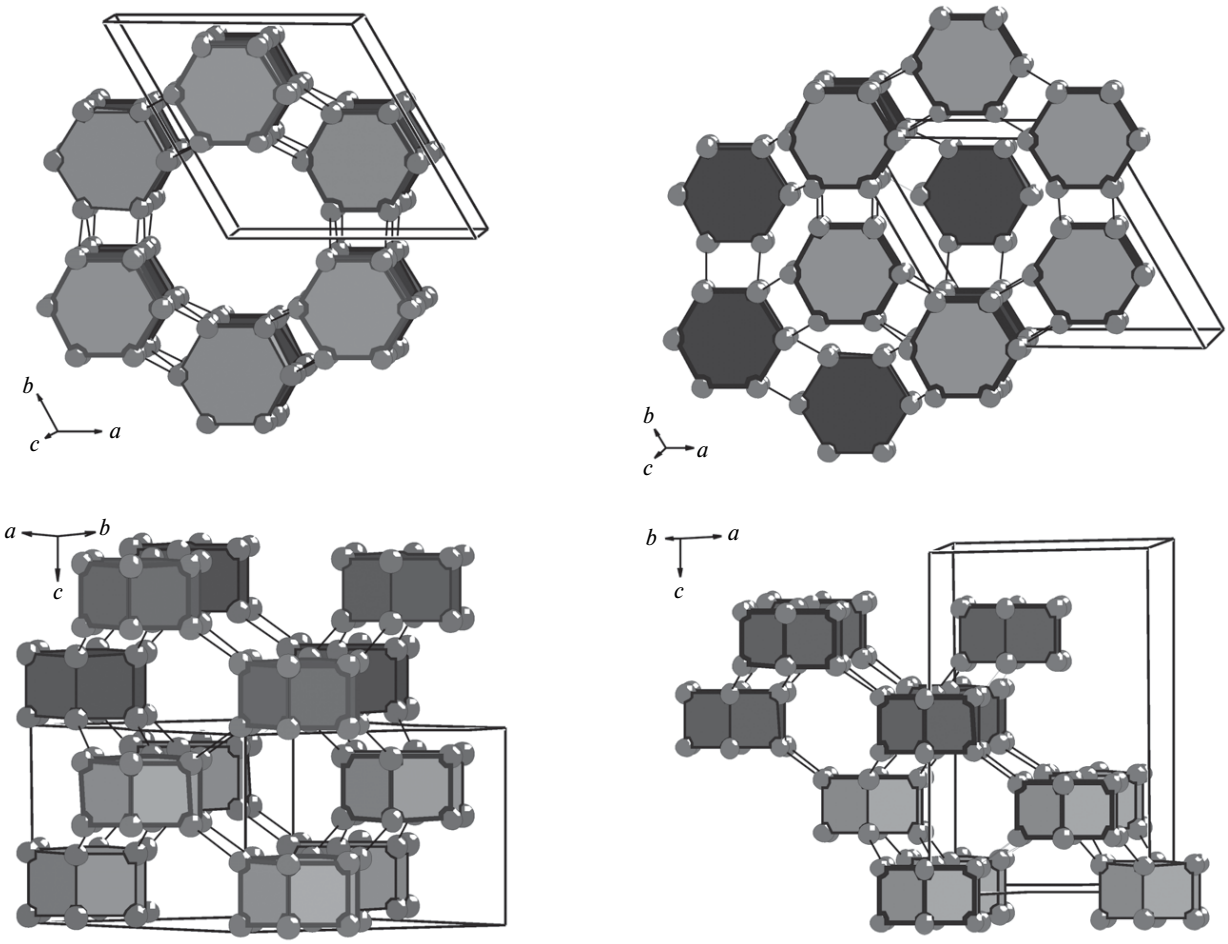

Fig. 7. Self-assembly of the **FR-5** framework, the **GME** structure type (a single-layer 1L structure).

Fig. 8. Self-assembly of the **FR-6** framework, the **AFX** structure type (two-layer packages, a 2L structure).

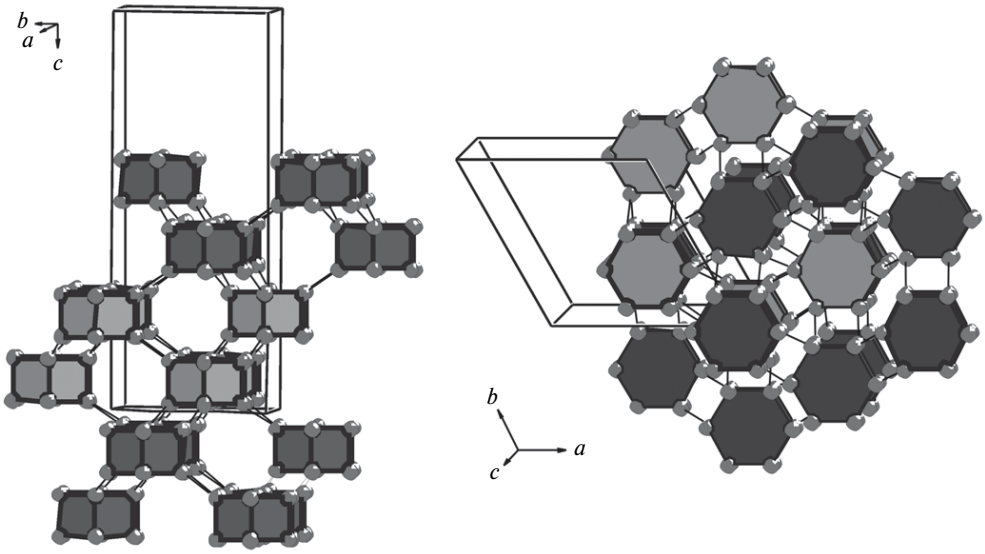

Fig. 9. Self-assembly of the **FR-7** framework, the **AFT** structure type (three-layer packages, a 3L structure).

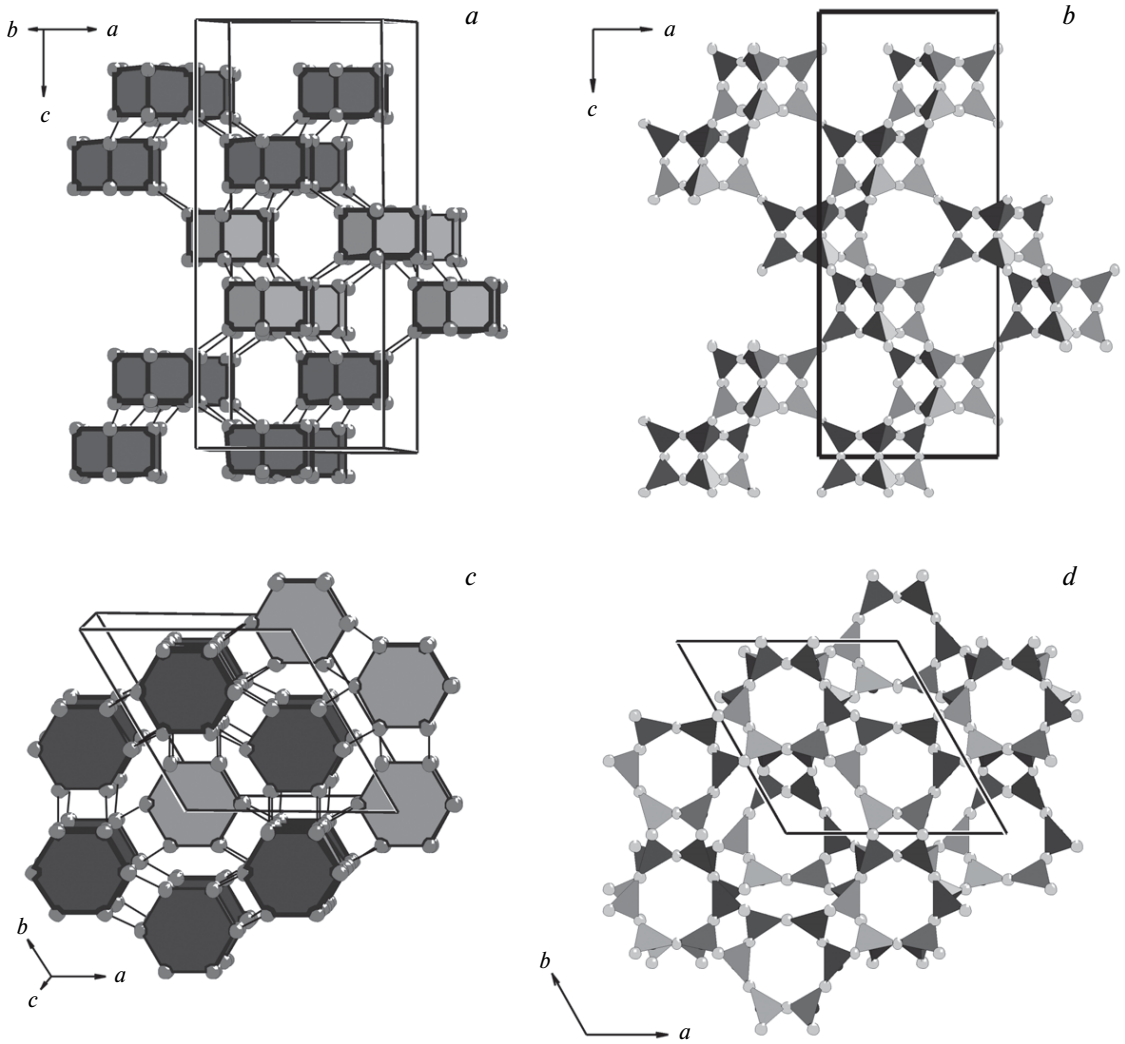

Fig. 10. Self-assembly of the **FR-8** framework (three-layer packages of hexamers, 3L-polytype). Projections of the framework along the *b* (*a*, *b*) and *c* (*c*, *d*) axes; the representation as connected T_{12} polyhedral 12-node clusters (*a*, *c*) and suprapolyhedral T clusters (*b*, *d*).

Table 2. Zeolite **FR-8 (ISC-2)** with the $T_{72}O_{144}$ framework. The coordinates and crystallographic positions of T and O atoms in the unit cell

Atom	Wyckoff position	Atomic coordinates		
		x	*y*	*z*
T(1)	12*o*	0.11000	0.44000	0.39000
T(2)	12*o*	0.11000	0.44000	0.28000
T(3)	12*o*	0.11000	0.44000	0.05000
T(4)	12*o*	0.00000	0.23000	0.45000
T(5)	12*o*	0.44000	0.11000	0.22000
T(6)	12*o*	0.44000	0.11000	0.11000
O(1)	6l	−0.89000	−0.33000	1.00000
O(2)	6*n*	−0.78000	−0.22000	0.95000
O(3)	12*o*	−0.61500	0.00000	0.92000
O(4)	6*n*	−0.55500	−0.11000	0.95000
O(5)	12*o*	−0.56000	0.33000	0.83500
O(6)	6*n*	−0.44500	0.44500	0.78000
O(7)	12*o*	−0.00000	0.61500	0.75000
O(8)	6*n*	−0.22000	0.56000	0.78000
O(9)	6*n*	−0.22000	0.56000	0.89000
O(10)	6*n*	−0.44500	0.44500	0.89000
O(11)	12*o*	0.11000	0.67000	0.66500
O(12)	6*n*	0.22000	0.78000	0.61000
O(13)	6*n*	0.22000	0.78000	0.72000
O(14)	6*n*	0.44500	0.89000	0.72000
O(15)	6*n*	0.44500	0.89000	0.61000
O(16)	12*o*	0.05500	−0.28000	0.58000
O(17)	6*m*	−0.23000	0	0.50000
O(18)	6*n*	−0.11500	0.11500	0.55000
O(19)	6*n*	−0.23000	−0.11500	0.45000

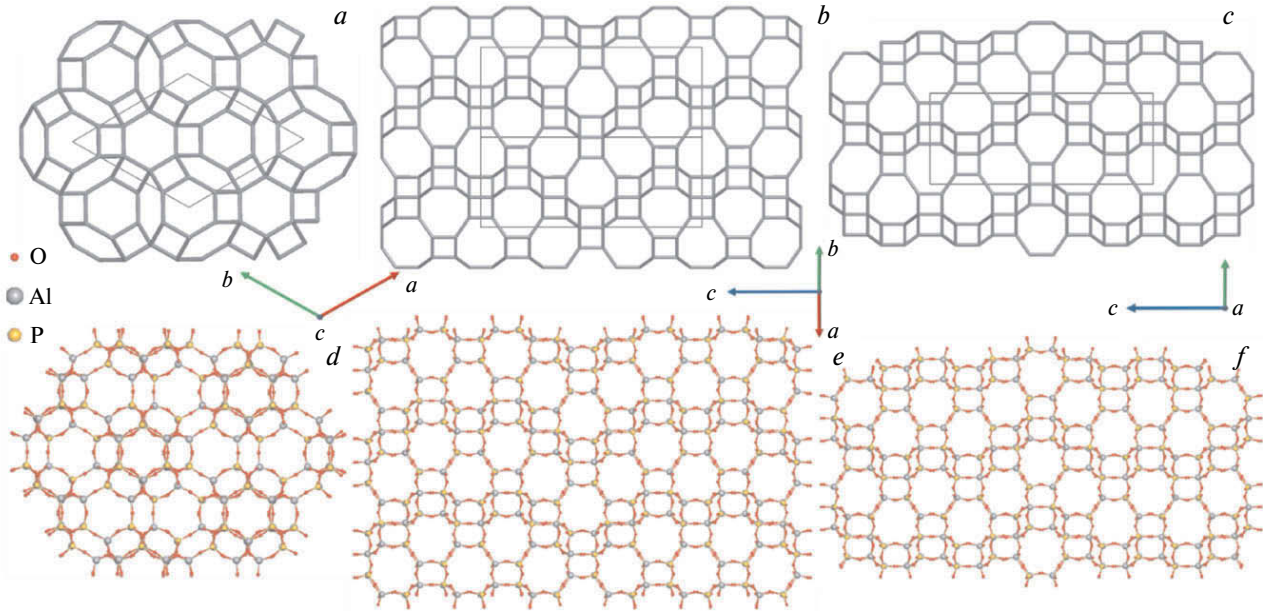

Fig. 11. The net of T atoms of hypothetical zeolite projected onto the (001) (*a*), (110) (*b*), and (100) (*c*) planes and the corresponding fragments of the framework (*d*—*f*).
Note. Figures 11—15 are available in full color in the on-line version of the journal (http://www.link.springer.com).

ISC-2, has no topological analogs among known zeolite frameworks. The crystallographic data for the **ISC-2** zeolite structure are as follows: a = 13.75 Å, c = 30.00 Å, V = 4912.0 Å^3, sp. gr. $P\bar{6}m2$ (No. 187). The coordinates and the crystallographic positions of the T and O atoms in the unit cell are given in Table 2. In the structure, the three-layer packages are related by translations along the z axis. Zeolite **ISC-2** is the 3L-polytype of the **GME** family.

A further analysis showed that 225 known framework types do not include more complex NL-polytypes of the **GME** family.

Analysis of a system of cavities in the ISC-2 structure

Initially, hypothetical zeolite **ISC-2** was modeled using the framework of the $AlPO_4$ composition. Then we constructed a three-periodic net with a given topology, the nodes of which were occupied by the corresponding atoms (Al, P, O). The geometry of the resulting framework was optimized (Fig. 11) by molecular mechanics implemented in the GULP program.[21] The standard potentials from the CATLOW library[22] were used as interatomic potentials.

The cavities and channels in the hypothetical zeolite were analyzed by means of the partition of the crystal space into certain polygons (tiles), which form the so-called natural tiling,[23] using the ToposPro program package.[20] From the physical point of view, tiles are the minimum intraframework cavities. The natural tiling is constructed using the following rules:[23]

1) the symmetry of the tiling should be the same as that of the net;

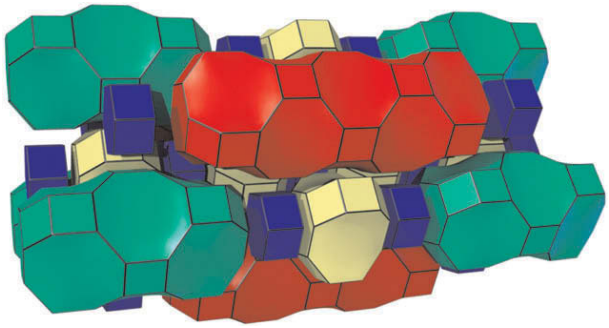

Fig. 12. Natural tiling of the net of hypothetical zeolite **ISC-2**.

2) the faces of the tiles are formed by strong rings, *i.e.*, the rings, which cannot be represented as a sum of smaller rings;

3) the tiles cannot include strong rings, which do not intersect with the rings of the same type;

4) if the intersecting rings differ in size, the smaller ring is taken as the face of the tile; if the intersecting rings have an equal size, they are not taken into account in choosing the faces of the tiles.

Currently, natural tilings are widely used for the search for and the description of the building blocks, as well as the schemes of assembling of zeolite frameworks.[1]

The partition of the net of the hypothetical zeolite gives a natural tiling (Fig. 12) composed of four types of tiles (Fig. 13, *a*—*d*): three tiles, which have been found earlier in the frameworks of known zeolites* (**t-hpr** [$4^6.6^2$],

* The classification of the tiles in zeolite frameworks is given in the study.[4]

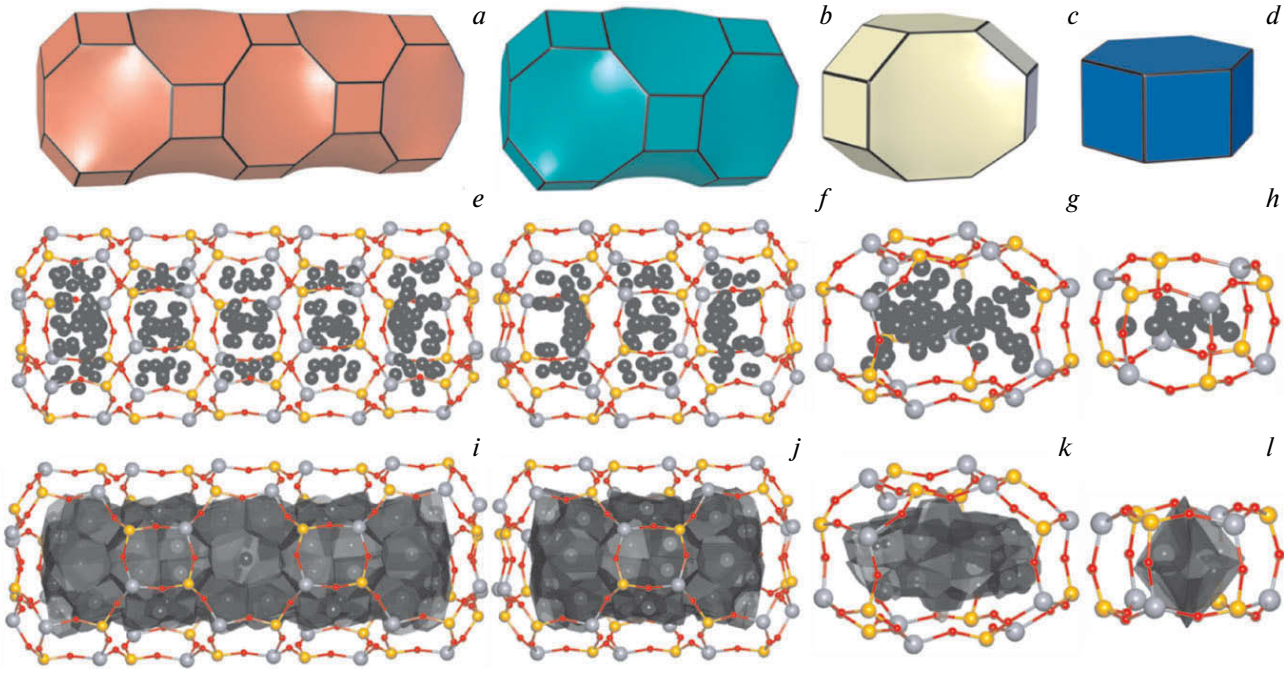

Fig. 13. The **t-isc-2** (*a*), **t-aft** (*b*), **t-gme** (*c*), and **t-hpr** (*d*) tiles and the corresponding structural fragments containing vertices of Voronoi—Dirichlet polyhedra (*e*—*h*) and intraframework cavities (*i*—*l*). The vertices of Voronoi—Dirichlet polyhedra and the intraframework cavities are in black.

t-gme [$4^9.6^2.8^3$], and **t-aft** [$4^{15}.6^2.8^9$]) and the tile with the [$4^{21}.6^2.8^{15}$] topology, which has not been described earlier (we called it **t-isc-2**) in a 6 : 4 : 1 : 1 ratio.

The face symbol of the [$4^{21}.6^2.8^{15}$] tile indicates that the tile has 21 four-membered rings, 2 six-membered rings, and 15 eight-membered rings as faces. It should be noted that the **t-hpr** tile is present in 30 framework types; **t-gme**, in 10 framework types; **t-aft**, in 2 framework types (AFT, AFX).[4]

The geometric characteristics of the cavities were calculated using an algorithm based on the Voronoi—Dirichlet partition.[24] This is a normal (face-to-face) partition of the crystal space formed by Voronoi—Dirichlet polyhedra (VDP) of all atoms of the structure. The VDP is a convex polyhedron, the faces of which are perpendicular to the segments connecting the central atom of the VDP to the surrounding atoms, where each face divides the corresponding segment into two halves. The algorithm of the VDP partition is implemented in the Dirichlet program of the ToposPro program package.

The algorithm of calculations of the geometric characteristics of the cavities involves the analysis of the vertices of VDPs constructed for atoms of the zeolite framework. Earlier, it has been shown[24] that the vertices of VDPs have a clear physical meaning. Since, according to the algorithm of the construction of VDPs, the latter occupy positions most remote from the atoms, VDPs can be represented as centers of depleted electron density regions (centers of elementary voids). It should be noted that this method treats only such vertices of VDPs that belong to a particular cavity in the framework corresponding to a certain tile (see Fig. 13, *e*—*h*).

The correspondence between the vertices of VDP (elementary voids) and the tile cavity is determined by the condition that all central atoms of VDP incident with this vertex belong to this tile.

In order to visualize and calculate the geometric parameters of the cavity, it is necessary, in turn, to construct VDP for each of the elementary voids that characterize the cavity taking into account both the atoms of the tile and other elementary voids. Since, when estimating the cavity size, we were interested in the opportunity of location of a particular molecule (organic structure-directing agent, OSDA) in this cavity, we used the modified method for the construction of VDPs, which takes into account the atom size. Thus, each face of VDP that separates the center of the elementary void and the atom of the tile is at a distance to this atom not smaller than the van der Waals radius of the latter. This, in turn, means that one should take into account only elementary voids that are at distances to the nearest framework atoms not smaller than the van der Walls radius of the latter (Fig. 14). This procedure gives the planes shown in Fig. 13, *i*—*l*.

The geometric characteristics of the cavity in the framework correspond to the characteristics of VDPs (see Fig. 13, *i*—*l*) calculated for the vertices of atomic VDPs, which meet the above-mentioned conditions. Hence, we calculated the volume and the shape (characterized by the

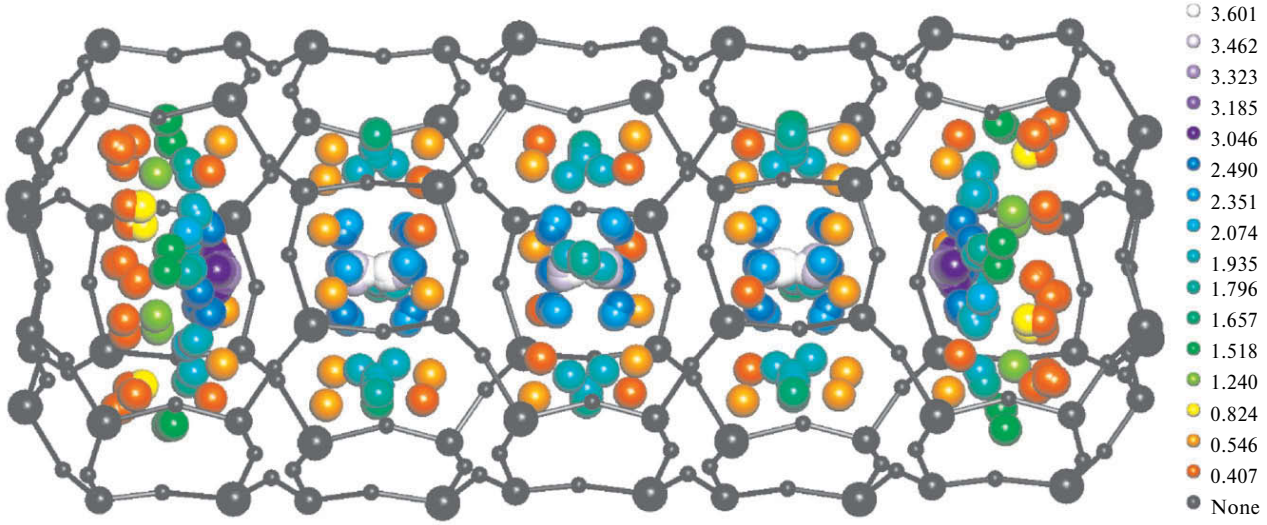

Fig. 14. Structural fragment corresponding to the **t-isc-2** tile. The vertices of Voronoi—Dirichlet polyhedra are colored in accordance with the distance to the nearest framework atom after deducing its van der Waals radius.

parameter G_3 and by the ratio of the principal moments of inertia of VDP, J_x/J_z and J_y/J_z) of all types of cavities in this framework (Table 3).

The search for potential structure-directing agents for the new type of the cavity, **t-isc-2**, was performed based on the criteria of the match between the volume and shape of the cavity and those of the structure-directing agent molecule. For this purpose, we created a database of topological types of molecules (TTM collection) that includes geometric and topological characteristics of more than 300000 different molecules obtained by analyzing the Cambridge Structural Database.[25] This approach revealed one of potential structure-directing agents (Fig. 15), the

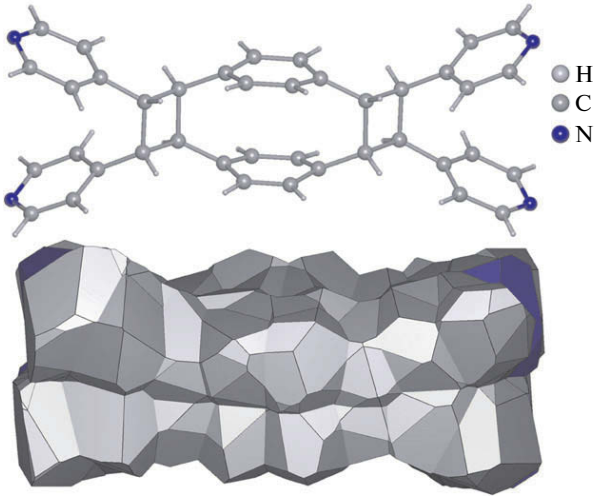

Fig. 15. Structure of the potential structure-directing agent for **ISC-2**: *a*, 3,4,11,12-tetrakis(4-pyridyl)pentacyclo-(12.2.2.2^{6,9}.0^{2,5}.0^{10,13})icosane-1(16),6,8,14,17,19-hexaene molecule;[26] *b*, its molecular Voronoi—Dirichlet polyhedron.

Table 3. Geometric characteristics of cavities in the framework of hypothetical zeolite **ISC-2**

Cavity type	V/Å^3	V*/Å^3	G_3	J_x/J_z	J_y/J_z
t-isc-2	844	1006	0.174	0.169	0.992
t-aft	469	596	0.104	0.408	0.982
t-gme	122	125	0.096	0.655	0.733
t-hpr	20	22	0.080	0.781	0.795

* The volume of the cavity taking into account the channels that link adjacent cavities.

geometric parameters of which (V = 712 Å^3, G_3 = 0.152, J_x/J_z = 0.215, J_y/J_z = 0.966) are in good agreement with the corresponding parameters of the cavity (see Table 3).

* * *

To summarize, we performed the combinatorial-topological modeling of the packings of symmetry-related T_{12} polyhedral clusters (hexagonal prisms), including the selection of underlying 2D microlayers, which are involved in the self-assembly of 3D framework structures of zeolites described by four-connected square T nets. It was found that all (four) combinatorially possible 3D framework structures correspond to real zeolite structures: **CHA** (mineral chabazite, $Ca_6(H_2O)_{40}Al_{12}Si_{24}O_{72}$), **AEI** (AlPO-18, $Al_{24}P_{24}O_{96}$,), **SAV** ($(C_{18}H_{42}N_6)_2(H_2O)_7Mg_5Al_{19}P_{24}O_{96}$), and **KFI** ($Na_{30}(H_2O)_{98}Al_{30}Si_{66}O_{192}$).

The modeling according to this scheme using a decorated underlying hexagonal net gives a family of polytype structures, the number of which is theoretically infinite due to three dufferent modes of the complementary arrangement of the layers linked to each other. The simplest 1L-, 2L-, and 3L-polytypes of this family correspond to

zeolites **GME** (gmelinite, $(Ca,Na)_4(H_2O)_{24}Al_8Si_{16}O_{48}$), **AFX** (SAPO-56, $H_3Al_{23}Si_5P_{20}O_{96}$), and **AFT** (AlPO-52, $Al_{36}P_{36}O_{144}$). In addition, one 3L-polytype corresponds to the new **ISC-2** framework, and it seems to be possible to produce the latter by selecting appropriate organic structure-directing agents (OSDA molecules) in order to stabilize the local regions corresponding to the largest cavities (**t-isc-2** tile). The examples of OSDA molecules, which were found using the specially created database of topological types of molecules (TTM collection), are given.

This study was financially supported by the Government of the Russian Federation (Project No. 14.V25.31.0005).

References

1. *The Zeolite Framework Database*, http://www.iza-structure.org/databases/.
2. J. V. Smith, *Chem. Rev*. 1988, **88**, 149.
3. J. V. Smith, in *Tetrahedral Frameworks of Zeolites, Clathrates and Related Materials*, Springer, Berlin, 2000.
4. N. A. Anurova, V. A. Blatov, G. D. Ilyushin, D. M. Proserpio, *J. Phys. Chem. C*, 2010, **114**, 10160.
5. V. A. Blatov, G. D. Ilyushin, D. M. Proserpio, *Chem. Mater.*, 2013, **25**, 412.
6. G. D. Ilyushin, V. A. Blatov, *Crystallogr. Rep*., 2012, **57**, 3.
7. M. V. Peskov, V. A. Blatov, G. D. Ilyushin, U. Schwingenschlцgl, *J. Phys. Chem. C*, 2012, **116**, 6734.
8. G. D. Ilyushin, V. A. Blatov, *Crystallogr. Rep*. (*Engl. Transl.*), 2013, **58**, 531 [*Kristallografiya*, 2013, **58**, 528].
9. G. D. Ilyushin, V. A. Blatov, *Crystallogr. Rep*. (*Engl. Transl.*), 2011, **56**, 75 [*Kristallografiya*, 2011, **56**, 80].
10. V. A. Blatov, G. D. Ilyushin *Crystallogr. Rep*. (*Engl. Transl.*), 2012, **57**, 360 [*Kristallografiya*, 2012, **57**, 415].
11. G. D. Ilyushin, V. A. Blatov, L. N. Dem´yanets, *Russ. J. Inorg. Chem*. (*Engl. Transl.*), 2011, **56**, 1570 [*Zh. Neorg. Khim.*, 2011, **56**, 1651].
12. G. D. Ilyushin, *Struct. Chem*., 2012, **23**, 997.
13. V. A. Blatov, G. D. Ilyushin, D. M. Proserpio, *Inorg. Chem*., 2011, **50**, 5714.
14. A. A. Pankova, V. A. Blatov, G. D. Ilyushin, D. M. Proserpio, *Inorg. Chem*., 2013, **52**, 13094.
15. G. D. Ilyushin, V. A. Blatov, *Russ. J. Inorg. Chem*. (*Engl. Transl.*), 2015, **60**, 469 [*Zh. Neorg. Khim*., 2015, **60**, 529].
16. V. Ya. Shevchenko, V. A. Blatov, G. D. Ilyushin, *Glass Phys. Chem*. (*Engl. Transl.*), 2013, **39**, 229 [*Fiz. Khim. Stekla*, 2013, **39**, 345].
17. V. Ya. Shevchenko, V. A. Blatov, G. D. Ilyushin, *Glass Phys. Chem*. (*Engl. Transl.*), 2013, **39**, 101 [*Fiz. Khim. Stekla*, 2013, **39**, 153].
18. V. Ya. Shevchenko, V. A. Blatov, G. D. Ilyushin, *Glass Phys. Chem*. (*Engl. Transl.*), 2014, **40**, 180 [*Fiz. Khim. Stekla*, 2014, **40**, 234].
19. V. A. Blatov, G. D. Ilyushin, A. E. Lapshin, O. Yu. Golubeva, *Glass Phys. Chem*. (*Engl. Transl.*), 2010, **36**, 663 [*Fiz. Khim. Stekla*, 2010, **36**, 843].
20. V. A. Blatov, A. P. Shevchenko, D. M. Proserpio, *Cryst. Growth Des.*, 2014, **14**, 3576, http://topospro.com.
21. J. D. Gale, *Z. Kristallogr*., 2005, **220**, 552.
22. J. D. Gale, N. J. Henson, *J. Chem. Soc., Faraday Trans*., 1994, **90**, 3175.
23. V. A. Blatov, O. Delgado-Friedrichs, M. O´Keeffe, D. M. Proserpio, *Acta Crystallogr.*, *Sect. A*, 2007, **63**, 418.
24. V. A. Blatov, *Cryst. Rev*., 2004, **10**, 249.
25. F. H. Allen, *Acta Crystallogr.*, *Sect. B*, 2002, **58**, 380.
26. T. Friscic, L. R. MacGillivray, *Chem. Commun*., 2003, 1306.

Received April 28, 2015